Heliyon 10 (2024) e32025

Contents lists available at ScienceDirect

Heliyon

journal homepage: www.cell.com/heliyon

Research article

Downregulation of DIP2B as a prognostic marker inhibited cancer proliferation and migration and was associated with immune infiltration in lung adenocarcinoma via CCND1 and MMP2

Chuang-Yan Wu [a,1], Zhao Liu [b,1], Wei-Min Luo [c,1], Huan Huang [d], Ni Jiang [e], Zhi-Peng Du [f], Fang-Ming Wang [a], Xu Han [f], Guan-Chao Ye [a], Qiang Guo [c,**], Jiu-Ling Chen [a,*]

[a] Department of Thoracic Surgery, Union Hospital, Tongji Medical College, Huazhong University of Science and Technology, Wuhan, China
[b] Cancer Center, Union Hospital, Tongji Medical College, Huazhong University of Science and Technology, Wuhan, China
[c] Department of Cardiothoracic Surgery, Taihe Hospital, Hubei University of Medicine, Shiyan, China
[d] Department of Thoracic Surgery, People's Hospital of Dongxihu, Wuhan, China
[e] Department of Obstetrics and Gynecology, Women and Children's Hospital of Chongqing Medical University, Chongqing, China
[f] Department of Gastroenterology, Tongji Hospital, Tongji Medical College, Huazhong University of Science and Technology, Wuhan, China

ARTICLE INFO

Keywords:
DIP2B
Biomarker
Lung adenocarcinoma
Immune microenvironment
Prognosis

ABSTRACT

Background: DIP2B is related to cancer progression. This study investigated the roles and pathways of DIP2B in lung adenocarcinoma (LUAD).

Methods: DIP2B expression and the relationship between survival time of cancer patients and DIP2B expression were analyzed. The relationship between DIP2B expression and survival time in LUAD patients was evaluated by a meta-analysis. Cox and survival analyses were used to evaluate the prognostic factors and construct a prognostic nomogram. The mechanisms and effects of DIP2B and the relationship between DIP2B expression and the immune microenvironment were investigated using bioinformatics, CCK-8, western blotting, and transwell experiments.

Results: DIP2B was overexpressed in LUAD tissues. DIP2B overexpression was associated with shorter prognosis and was an unfavorable risk factor for prognosis in LUAD patients. DIP2B co-expressed genes were involved in cell division, DNA repair, cell cycle, and others. Inhibition of DIP2B expression could downregulate the proliferation, migration, and invasion of LUAD A549 and H1299 cells, which was related to the decrease in CCND1 and MMP2 protein expression. BRCA1 overexpression was associated with short prognosis, and the nomogram formed by DIP2B and BRCA1 was associated with a poor prognosis in LUAD patients. DIP2B expression correlated with immune cells (such as CD8 T cells, Tcm, and iDCs) and cell markers.

Conclusion: DIP2B is a potential biomarker of poor prognosis and the immune microenvironment in LUAD. Inhibition of DIP2B expression downregulated cancer cell proliferation, migration, and invasion, which might be related to the decrease in CCND1 and MMP2 protein expression. DIP2B-related nomograms might be useful tools for predicting the prognosis of LUAD patients.

* Corresponding author.
** Corresponding author.
E-mail addresses: guoqianglidan2024@hbmu.edu.cn (Q. Guo), jiulingchen@hust.edu.cn (J.-L. Chen).
[1] Chuang-Yan Wu, Zhao Liu, and Wei-Min Luo stands for co-first author.

https://doi.org/10.1016/j.heliyon.2024.e32025
Received 4 May 2023; Received in revised form 22 May 2024; Accepted 27 May 2024
Available online 28 May 2024

1. Introduction

The incidence and death of non-small cell lung cancer (NSCLC) patients remains high [1,2]. Lung adenocarcinoma (LUAD) is one of the common subtypes of NSCLC. Patients with early-stage LUAD achieve a good long-term prognosis after early diagnosis and surgery, while some patients with advanced LUAD have a poor prognosis. At present, gene mutation detection in the tumor tissues of advanced LUAD and treatment targeting the mutation sites could improve the long-term prognosis of lung cancer patients [3,4]. However, the survival time of these LUAD patients remains suboptimal [1,2], so identifying new targets is needed to improve the prognosis of LUAD patients.

The protein encoded by the disco interacting protein 2 homolog B (DIP2B) gene contains a binding site for the transcriptional regulator DNA methyltransferase 1-related protein 1 and an AMP-binding site. DIP2B is associated with cancer progression and lung development [5–8]. Moreover, cell proliferation, migration, and invasion abilities are restricted when DIP2B expression is inhibited in human colon cancer RKO and SW620 cells. Furthermore, β-catenin, vimentin, and Snail protein levels decreased after inhibiting DIP2B expression in cancer cells [6]. During embryogenesis, abnormal DIP2B expression results in intrauterine growth restriction, impaired lung formation, and perinatal mortality [7]. DIP2B plays a crucial role in late lung maturation, as loss of DIP2B results in disruption of air sac formation, increased interstitial compartmentalization, and increased cellularity, as well as enhanced cellular proliferative capacity during the cystic stage of lung development [7]. Currently, the roles and signaling mechanisms of DIP2B in LUAD are unknown. Therefore, this study investigated the relationship between DIP2B expression in the prognosis of cancer patients and cancer immune infiltration using bioinformatics to provide a new candidate marker for the treatment of LUAD.

2. Materials and methods

2.1. Gene expression data and general clinical profile of LUAD patients

DIP2B gene expression data of the Fragments Per Kilobase of exon model per Million mapped fragments (FPKM) type were retrieved from The Cancer Genome Atlas (TCGA (https://portal.gdc.cancer.gov/)) database, of which there were 59 normal tissue samples and 535 LUAD tissue samples [9]. The clinical data of cancer patients were downloaded, and the age, sex, pathological stage, T stage, N stage, M stage, and other data of cancer patients were extracted from the TCGA database. In addition, normal and cancerous tissues were collected from 10 LUAD patients, and the expression levels of DIP2B were determined through immunohistochemistry and western blotting. Written informed consent was obtained from all LUAD patients, and this study was approved by the Ethics Committee of Huazhong University of Science and Technology.

2.2. The expression levels of DIP2B in clinical tissues using IHC

Following fixation and treatment with high-temperature dewaxing and hydration, antigen retrieval was performed, followed by blocking of nonspecific binding utilizing sheep serum albumin. Incubation with the DIP2B antibody and the horseradish peroxidase (HRP)-conjugated secondary antibody was carried out, with washing performed to remove impurities. DAB staining was applied, followed by restaining with hematoxylin. The slides were then washed and mounted [10]. Finally, the stained tissues were observed and analyzed under a microscope, and the images were recorded. In addition, the standard process of immunoblotting was followed to detect the expression level of DIP2B in LUAD, and the DIP2B antibody (863713, ZENBIO, China) concentration was 1:1000 [10].

2.3. Lung cancer explorer (LCE) database

The LCE (http://lce.biohpc.swmed.edu/) database uses meta-analysis to effectively integrate the results of the datasets in the TCGA and GEO databases, which is more reliable than a single dataset [11]. The relationship between DIP2B expression and survival time of LUAD patients was visualized using the meta-analysis in the LCE database.

2.4. The relationship between DIP2B overexpression and prognostic indicators

The expression of DIP2B in LUAD tissues of FPKM type was identified, and according to age, sex, pathological stage, T stage, N stage, M stage and others, the DIP2B expression levels were determined in LUAD tissues. In addition, whether there were significant differences in the age, sex, pathological stage, T stage, N stage, and M stage of the patients in each group was determined after grouping by the median value of DIP2B. Kaplan–Meier (K–M) survival analysis was used to show the relationship between DIP2B expression level and overall survival (OS), progression-free survival (PFI), and disease-specific survival (DSS) in subgroups of LUAD patients based on age, sex, pathological stage, T stage, N stage, M stage, etc [12,13].

2.5. Construction of DIP2B-related nomograms

The relationship between T stage, N stage, M stage, pathological stage, sex, age, smoking history, and DIP2B expression and prognosis (OS, DSS, and PFI) in patients with LUAD was assessed using univariate Cox regression analysis and multivariate Cox analysis ($P < 0.05$) [12,13]. DIP2B-related nomograms were constructed to understand the OS, DSS, and PFI of LUAD patients based on

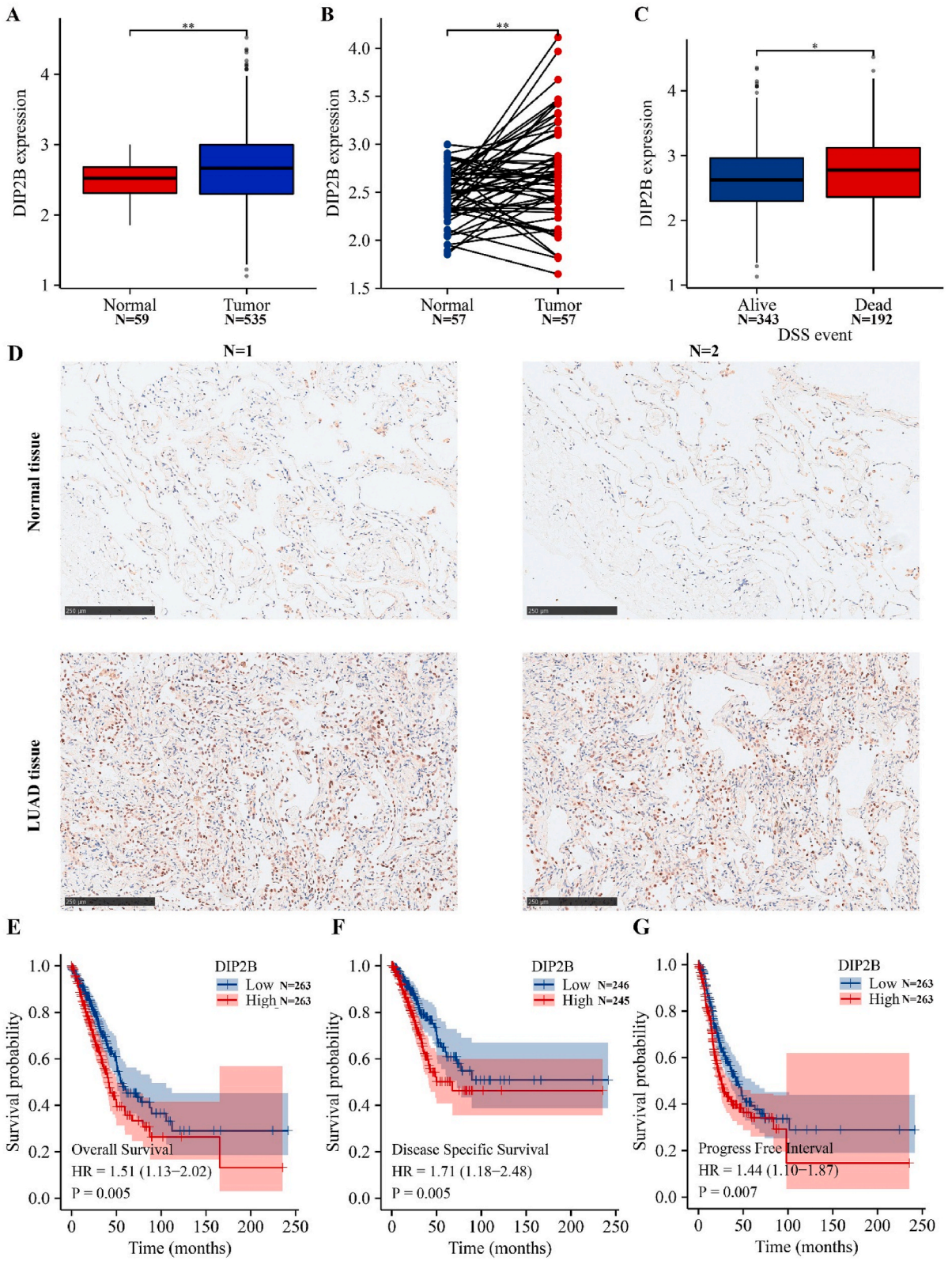

(caption on next page)

Fig. 1. DIP2B overexpression predicted a shorter prognosis in LUAD. (A–B) DIP2B expression in LUAD tissues using the Wilcoxon rank sum test; (C) DIP2B expression in cancer tissues at the DSS event using the Wilcoxon rank sum test; (D) DIP2B overexpression in clinical LUAD tissues using immunohistochemistry; (E–G) DIP2B expression in the prognosis of LUAD patients using K−M survival analysis. Note: LUAD, lung adenocarcinoma; PFI, progression-free survival; OS, overall survival; DSS, disease-specific survival; K−M, Kaplan−Meier; *, $P < 0.05$; **, $P < 0.01$.

the multivariate Cox analysis results, and were verified using calibration curve.

2.6. Extraction of DIP2B co-expressed genes

The correlation between genes was displayed by the correlation coefficient, and the closer the coefficient was to plus or minus 1, the stronger the correlation. DIP2B co-expressed genes were displayed by using Pearson correlation analysis in 535 LUAD tissues [9], and the co-expressed genes were filtered by an absolute correlation coefficient of 0.5 and $P < 0.001$.

2.7. The roles and signaling pathways of DIP2B co-expressed genes

Gene Ontology (GO) annotation and Kyoto Encyclopedia of Genes and Genomes (KEGG) analysis indicate the biological functions and signaling pathways involved in multiple genes [14,15]. The biological processes, molecular functions, and cellular components involved in DIP2B co-expressed genes were investigated using GO annotation, and the signaling pathways of DIP2B co-expressed gene enrichment were investigated by KEGG in the DAVID (https://david.ncifcrf.gov/) database.

Table 1
DIP2B expression in cancer tissues based on clinical features using T test and one-way ANOVA.

Features	Low expression	High expression	P
N	267	268	
T stage			0.124
T1	99 (18.6 %)	76 (14.3 %)	
T2	139 (26.1 %)	150 (28.2 %)	
T3	21 (3.9 %)	28 (5.3 %)	
T4	7 (1.3 %)	12 (2.3 %)	
N stage			0.232
N0	172 (33.1 %)	176 (33.9 %)	
N1	55 (10.6 %)	40 (7.7 %)	
N2	32 (6.2 %)	42 (8.1 %)	
N3	1 (0.2 %)	1 (0.2 %)	
M stage			0.161
M0	190 (49.2 %)	171 (44.3 %)	
M1	9 (2.3 %)	16 (4.1 %)	
Pathologic stage			0.386
Stage I	150 (28.5 %)	144 (27.3 %)	
Stage II	63 (12 %)	60 (11.4 %)	
Stage III	39 (7.4 %)	45 (8.5 %)	
Stage IV	9 (1.7 %)	17 (3.2 %)	
Gender			0.129
Female	152 (28.4 %)	134 (25 %)	
Male	115 (21.5 %)	134 (25 %)	
Age			0.291
≤65	121 (23.4 %)	134 (26 %)	
>65	137 (26.6 %)	124 (24 %)	
Residual tumor			0.350
R0	184 (49.5 %)	171 (46 %)	
R1	5 (1.3 %)	8 (2.2 %)	
R2	1 (0.3 %)	3 (0.8 %)	
Smoker			0.681
No	39 (7.5 %)	36 (6.9 %)	
Yes	217 (41.7 %)	229 (44 %)	
OS event			0.041
Alive	183 (34.2 %)	160 (29.9 %)	
Dead	84 (15.7 %)	108 (20.2 %)	
DSS event			0.017
Alive	201 (40.3 %)	178 (35.7 %)	
Dead	48 (9.6 %)	72 (14.4 %)	
PFI event			0.104
Alive	164 (30.7 %)	145 (27.1 %)	
Dead	103 (19.3 %)	123 (23 %)	

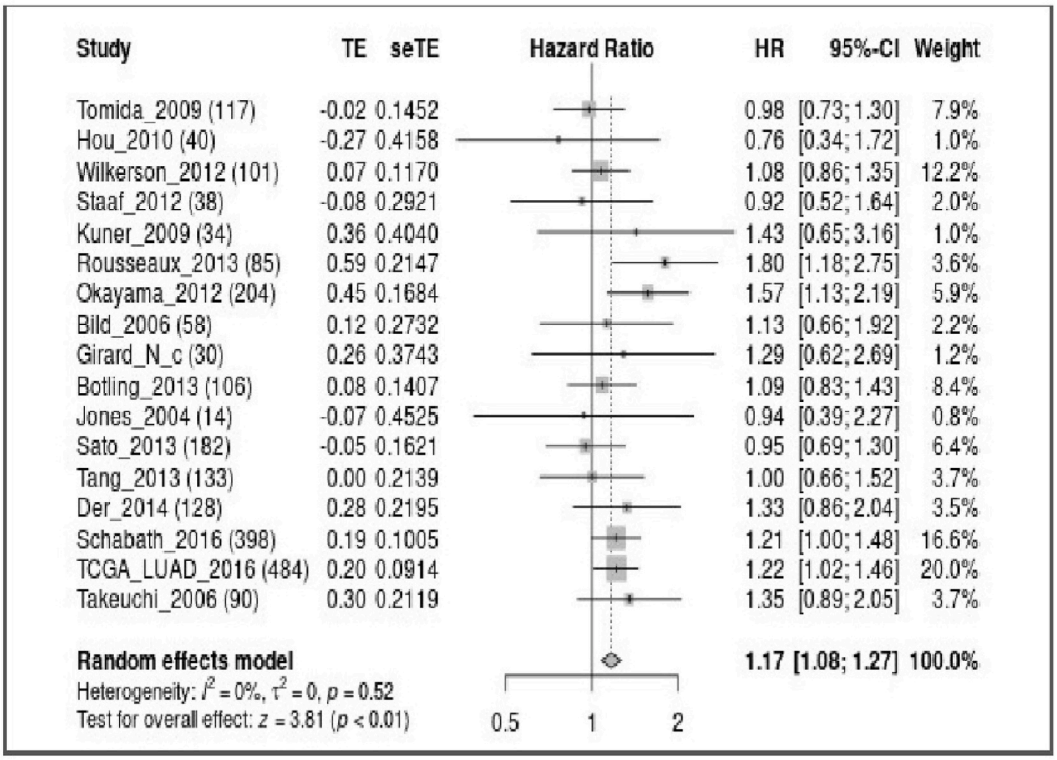

Fig. 2. DIP2B overexpression is related to the shorter OS of LUAD patients via meta-analysis in the LCE database. Note: LUAD, lung adenocarcinoma; OS, overall survival; LCE, Lung Cancer Explorer.

2.8. The relationship between DIP2B and key genes of the protein–protein interaction (PPI) network

The PPI network of DIP2B co-expressed genes was constructed and was further displayed with a binding score of 0.7 in the STRING database. In addition, visual network analysis was performed using Cytoscape (version: 3.8.2) software, and the CytoHubba plugin was used to obtain the ten key genes [9]. The relationship between DIP2B expression levels and the expression of BRCA1, EP300, BPTF, NIPBL, RPS28, RPS8, RPS11, RPS9, RPS14, and AGO2 was shown by Pearson correlation analysis.

2.9. Construction of nomograms of DIP2B and BRCA1

The relationship between BRCA1, EP300, BPTF, NIPBL, RPS28, RPS8, RPS11, RPS9, RPS14, and AGO2 expression and OS, DSS, and PFI in LUAD patients was explored by K–M survival analysis grouped by the median values of BRCA1, EP300, BPTF, NIPBL, RPS28, RPS8, RPS11, RPS9, RPS14, and AGO2 expression. The nomograms of DIP2B co-expressed genes were constructed based on the survival analysis results, and were verified using calibration curve.

2.10. The relationship between DIP2B overexpression and the immune microenvironment

The expression of immune cells in the tissues of LUAD patients was analyzed using the single sample gene set enrichment analysis (ssGSEA) method [16,17]. Pearson correlation analysis was used to investigate the relationship between DIP2B expression and immune cells and immune cell markers.

2.11. Construction of the LUAD cell models that inhibited DIP2B expression

A549 and H1299 cells were grown in RPMI-1640 medium with 10 % fetal bovine serum (FBS) and 1 % penicillin–streptomycin before transfection according to the standard procedure [13]. The expression of DIP2B protein in the control cells and interfering DIP2B-expressing cells was detected by western blotting 24 h after transfection. Total protein was extracted from the control group and the interference DIP2B expression groups and separated by gel electrophoresis after BCA quantification using a 1:1000 DIP2B antibody (863713, ZENBIO, China), 1:3000 GAPDH antibody (ab37168, Abcam, UK) and 1:3000 secondary antibody (111-035-003, Jackson, China) [18]. The siRNA sequence of DIP2B was obtained from Guangzhou Ruibo Company (China). The two interfering sequences of DIP2B were si-DIP2B-1: GCTACTGGATTGGCTGTA GAA and si-DIP2B-2: GAAGAGCATTACCTCATCGTT.

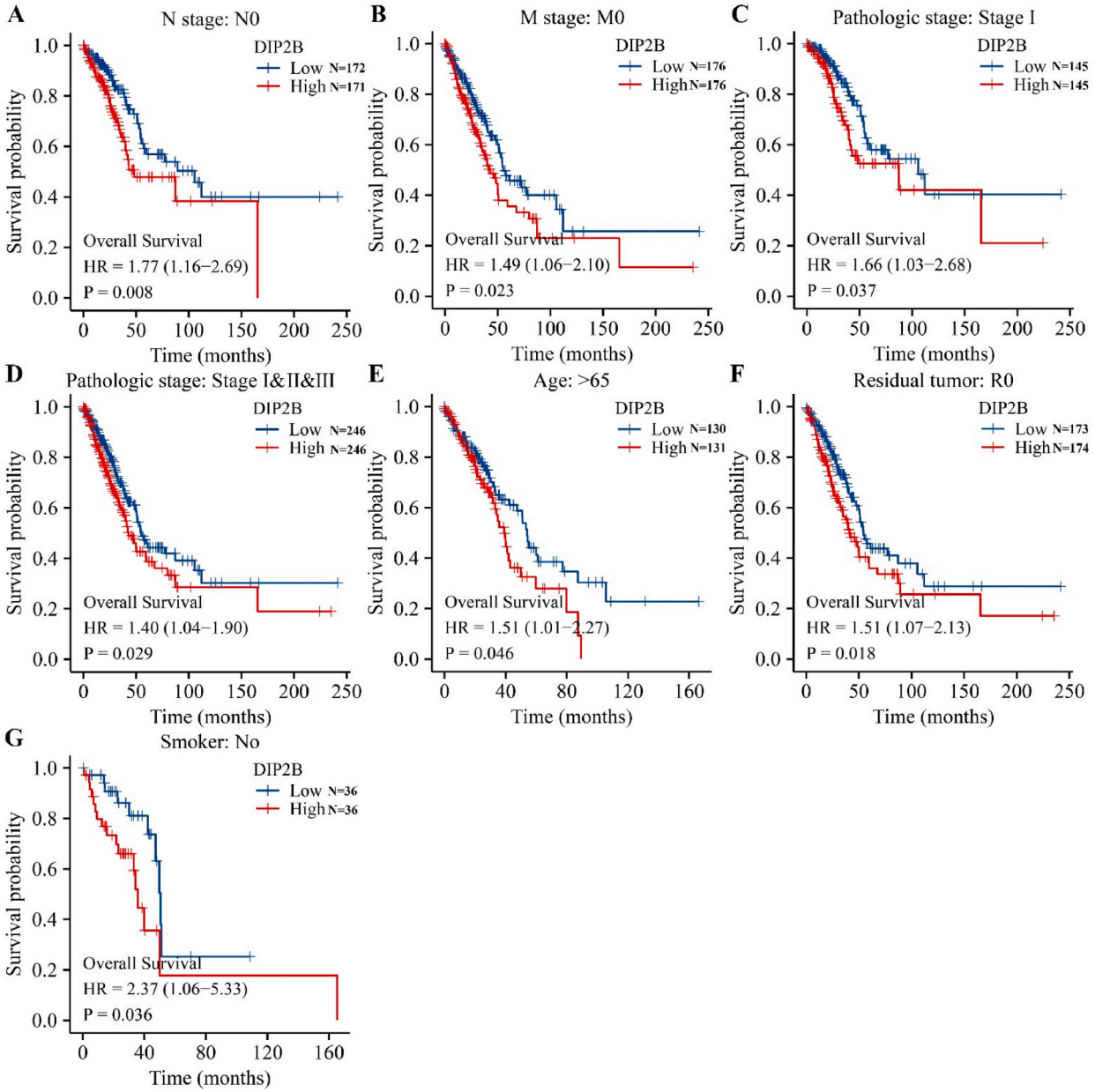

Fig. 3. DIP2B overexpression was associated with OS in a subgroup of LUAD patients via K–M survival analysis. (A) N0; (B) M0; (C) Stage I; (D) Stage I-III; (E) Age (>65); (F) R0; (G) No smoking history. Note: LUAD, lung adenocarcinoma; OS, overall survival; K–M, Kaplan–Meier.

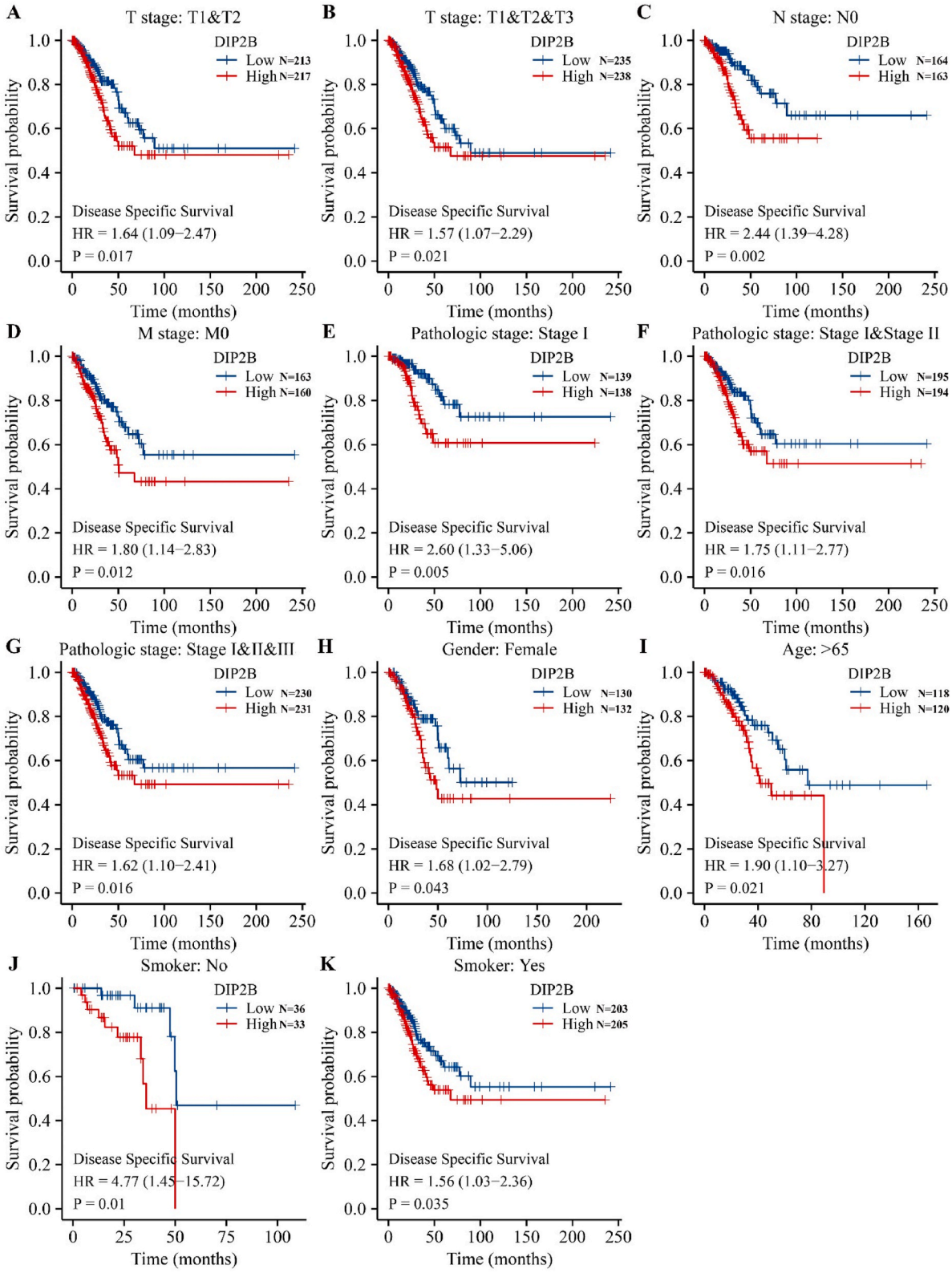

Fig. 4. DIP2B overexpression was associated with the DSS of subgroup LUAD patients via K–M survival analysis. (A) T1-2; (B) T1-3; (C) N0; (D) M0; (E) Stage I; (F) Stage I-II; (G) Stage I-III; (H) Female; (I) Age (>65); (J) No smoking history; (K) Smoking history. Note: LUAD, lung adenocarcinoma; DSS, disease-specific survival; K–M, Kaplan–Meier.

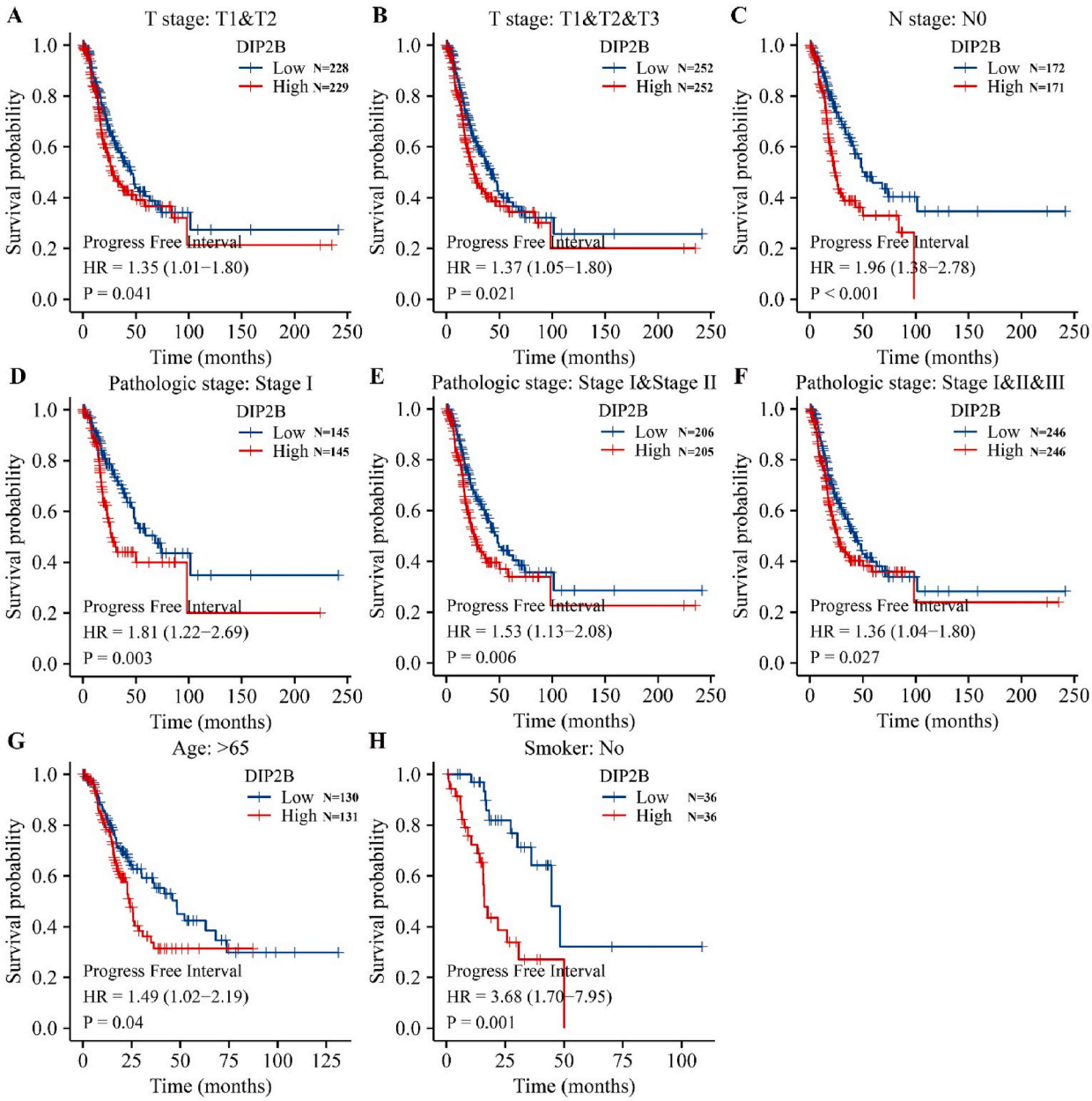

Fig. 5. DIP2B overexpression was associated with the PFI of subgroup LUAD patients via K−M survival analysis. (A) T1-2; (B) T1-3; (C) N0; (D) Stage I; (E) Stage I-II; (F) Stage I-III; (G) Age (>65); (H) No smoking history. Note: LUAD, lung adenocarcinoma; PFI, progression-free survival; K−M, Kaplan−Meier.

Table 2
Cox regression analysis showed the risk factors for short OS in LUAD.

Characteristics	N	HR (95 % CI)	P value	HR (95 % CI)	P value
T stage	523				
T1	175	Reference			
T2	282	1.521 (1.068–2.166)	0.020	1.571 (0.998–2.473)	0.051
T3	47	2.937 (1.746–4.941)	<0.001	3.499 (1.724–7.103)	<0.001
T4	19	3.326 (1.751–6.316)	<0.001	1.805 (0.813–4.006)	0.147
N stage	510				
N0	343	Reference			
N1	94	2.381 (1.695–3.346)	<0.001	2.321 (1.217–4.427)	0.011
N2	71	3.108 (2.136–4.521)	<0.001	1.841 (0.758–4.474)	0.178
N3	2	0.000 (0.000-Inf)	0.994	0.000 (0.000-Inf)	0.993
M stage	377				
M0	352	Reference			
M1	25	2.136 (1.248–3.653)	0.006	1.836 (0.831–4.056)	0.133
Pathologic stage	518				
Stage I	290	Reference			
Stage II	121	2.418 (1.691–3.457)	<0.001	0.852 (0.426–1.704)	0.651
Stage III	81	3.544 (2.437–5.154)	<0.001	1.577 (0.593–4.192)	0.362
Stage IV	26	3.790 (2.193–6.548)	<0.001		
Gender	526				
Female	280	Reference			
Male	246	1.070 (0.803–1.426)	0.642		
Age	516				
≤65	255	Reference			
>65	261	1.223 (0.916–1.635)	0.172		
Smoker	512				
No	72	Reference			
Yes	440	0.894 (0.592–1.348)	0.591		
DIP2B	526				
Low	263	Reference			
High	263	1.512 (1.131–2.021)	0.005	1.494 (1.065–2.095)	0.020

Note: LUAD, lung adenocarcinoma; OS, overall survival; HR, hazard ratio; CI, confidence interval.

Table 3
Cox regression analysis showed the risk factors for short DSS in LUAD.

Characteristics	N	HR (95 % CI)	P value	HR (95 % CI)	P value
T stage	488				
T1	168	Reference			
T2	262	1.701 (1.085–2.668)	0.021	1.642 (0.924–2.917)	0.091
T3	43	2.846 (1.453–5.572)	0.002	3.194 (1.211–8.422)	0.019
T4	15	2.770 (1.061–7.230)	0.037	1.753 (0.569–5.402)	0.328
N stage	475				
N0	327	Reference			
N1	83	2.751 (1.808–4.185)	<0.001	2.508 (1.091–5.769)	0.030
N2	63	2.762 (1.698–4.493)	<0.001	1.774 (0.513–6.133)	0.365
N3	2	0.000 (0.000-Inf)	0.995	0.000 (0.000-Inf)	0.996
M stage	344				
M0	323	Reference			
M1	21	2.455 (1.269–4.749)	0.008	2.410 (0.981–5.921)	0.055
Pathologic stage	483				
Stage I	277	Reference			
Stage II	112	3.017 (1.931–4.715)	<0.001	0.885 (0.358–2.189)	0.791
Stage III	72	3.326 (2.028–5.457)	<0.001	1.367 (0.349–5.364)	0.654
Stage IV	22	4.632 (2.371–9.050)	<0.001		
Gender	491				
Female	262	Reference			
Male	229	0.989 (0.687–1.424)	0.954		
Age	481				
≤65	243	Reference			
>65	238	1.013 (0.701–1.464)	0.944		
Smoker	477				
No	69	Reference			
Yes	408	1.040 (0.602–1.796)	0.889		
DIP2B	491				
Low	246	Reference			
High	245	1.711 (1.180–2.481)	0.005	1.896 (1.215–2.958)	0.005

Note: LUAD, lung adenocarcinoma; DSS, disease-specific survival; HR, hazard ratio; CI, confidence interval.

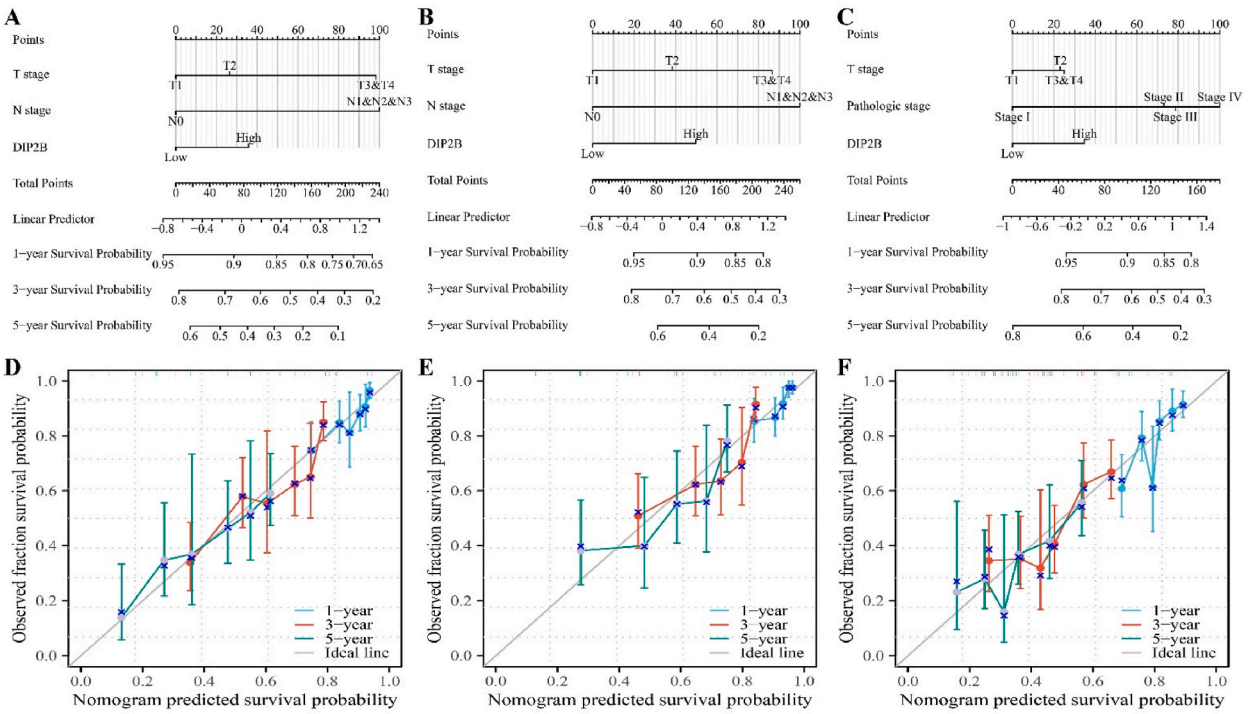

Fig. 6. The nomogram based on T stage, N stage, M stage and DIP2B expression predicted the total survival time of LUAD patients at 1-, 3- and 5-years. (A) OS-related nomogram; (B) DSS-related nomogram; (C) PFI-related nomogram; (D–F) The calibration curves of nomogram in OS, DSS, and PFI. Note: LUAD, lung adenocarcinoma; PFI, progression-free survival; OS, overall survival; DSS, disease-specific survival.

Table 4
Cox regression analysis showed the risk factors for a short PFI in LUAD.

Characteristics	N	HR (95 % CI)	P value	HR (95 % CI)	P value
T stage	523				
T1	175	Reference			
T2	282	1.758 (1.276–2.422)	<0.001	1.548 (1.116–2.146)	0.009
T3	47	3.495 (2.199–5.556)	<0.001	2.668 (1.452–4.904)	0.002
T4	19	1.113 (0.444–2.791)	0.819	0.451 (0.149–1.367)	0.159
N stage	510				
N0	343	Reference			
N1	94	1.540 (1.118–2.122)	0.008	1.258 (0.712–2.221)	0.429
N2	71	1.498 (1.018–2.205)	0.040	0.455 (0.156–1.327)	0.149
N3	2	0.906 (0.127–6.485)	0.922	0.646 (0.072–5.756)	0.695
M stage	377				
M0	352	Reference			
M1	25	1.513 (0.855–2.676)	0.155		
Pathologic stage	518				
Stage I	290	Reference			
Stage II	121	2.013 (1.478–2.742)	<0.001	1.273 (0.717–2.261)	0.410
Stage III	81	1.831 (1.257–2.669)	0.002	3.236 (1.052–9.952)	0.040
Stage IV	26	2.086 (1.189–3.657)	0.010	2.126 (1.073–4.213)	0.031
Gender	526				
Female	280	Reference			
Male	246	1.172 (0.901–1.526)	0.236		
Age	516				
≤65	255	Reference			
>65	261	1.023 (0.784–1.335)	0.867		
Smoker	512				
No	72	Reference			
Yes	440	0.968 (0.658–1.426)	0.870		
DIP2B	526				
Low	263	Reference			
High	263	1.438 (1.103–1.874)	0.007	1.412 (1.076–1.854)	0.013

Note: LUAD, lung adenocarcinoma; PFI, progression-free survival; HR, hazard ratio; CI, confidence interval.

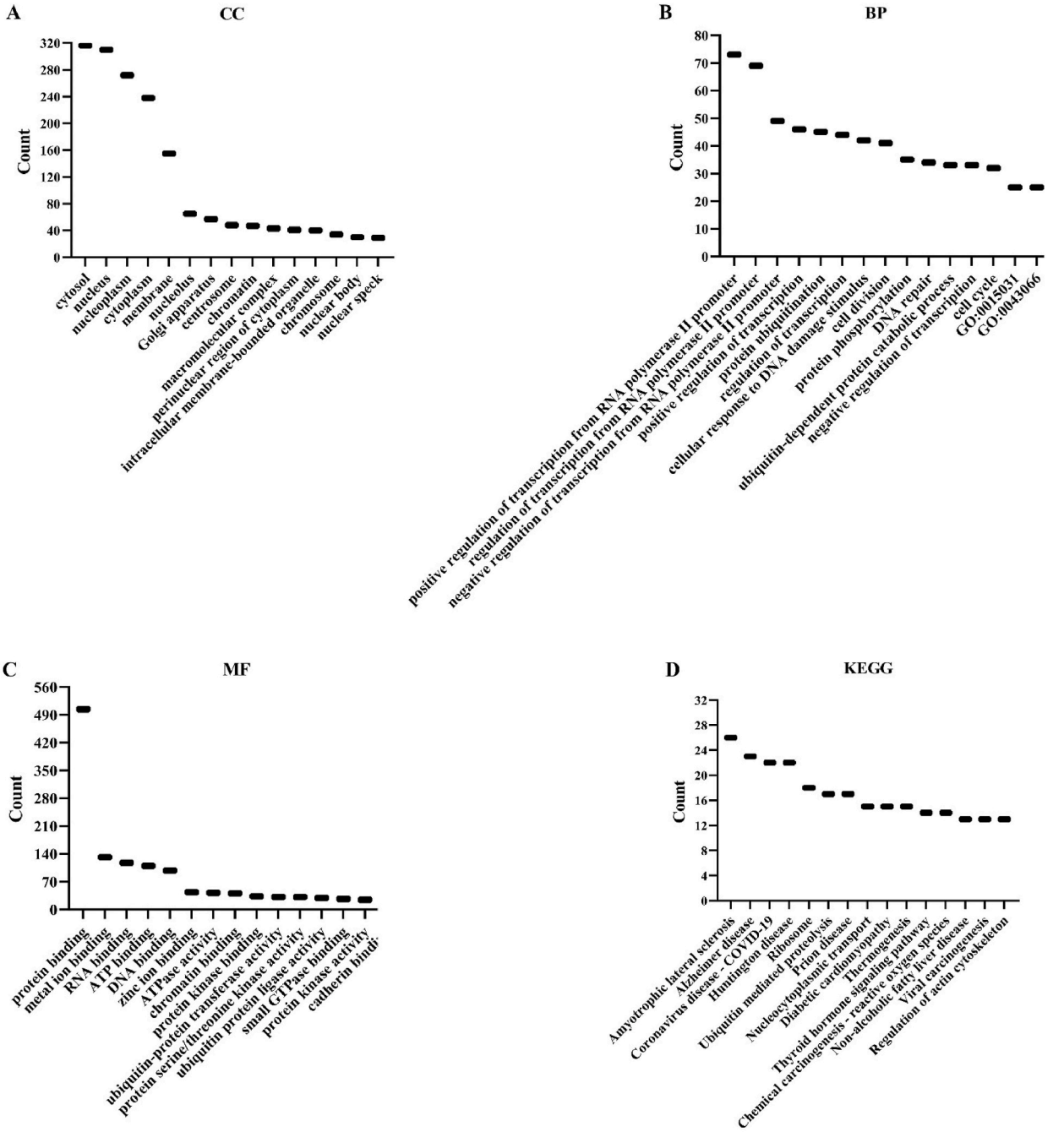

Fig. 7. Functions and mechanisms of DIP2B co-expressed genes via GO and KEGG analysis. (A) CC; (B) MF; (C) MF; (D) KEGG. Note: KEGG, Kyoto Encyclopedia of Genes and Genomes; BP, biological processes; GO, Gene Ontology; CC, cellular components; MF, molecular function.

Table 5
Signaling pathways of DIP2B co-expressed genes via KEGG analysis.

Term	Signaling pathways	Count	P
hsa03013	Nucleocytoplasmic transport	15	7.56E-06
hsa03010	Ribosome	18	1.05E-05
hsa04120	Ubiquitin mediated proteolysis	17	1.06E-05
hsa05171	Coronavirus disease-COVID-19	22	1.46E-05
hsa04919	Thyroid hormone signaling pathway	14	1.18E-04
hsa05014	Amyotrophic lateral sclerosis	26	2.31E-04
hsa05016	Huntington disease	22	7.43E-04
hsa04932	Non-alcoholic fatty liver disease	13	0.00388381
hsa05415	Diabetic cardiomyopathy	15	0.005274211
hsa05010	Alzheimer disease	23	0.005517511
hsa05211	Renal cell carcinoma	8	0.006172256
hsa01522	Endocrine resistance	9	0.012717532
hsa05020	Prion disease	17	0.013559892
hsa03250	Viral life cycle - HIV-1	7	0.014738879
hsa00310	Lysine degradation	7	0.014738879
hsa04714	Thermogenesis	15	0.016133895
hsa04012	ErbB signaling pathway	8	0.018415845
hsa05224	Breast cancer	11	0.018908202
hsa04110	Cell cycle	10	0.019070938
hsa04130	SNARE interactions in vesicular transport	5	0.019971302
hsa05208	Chemical carcinogenesis - reactive oxygen species	14	0.026105825
hsa05203	Viral carcinogenesis	13	0.029878198
hsa05220	Chronic myeloid leukemia	7	0.033786043
hsa05215	Prostate cancer	8	0.034874221
hsa05213	Endometrial cancer	6	0.036821505
hsa01521	EGFR tyrosine kinase inhibitor resistance	7	0.039742744
hsa05225	Hepatocellular carcinoma	11	0.042135623
hsa04810	Regulation of actin cytoskeleton	13	0.046038198

Note: KEGG, Kyoto Encyclopedia of Genes and Genomes.

2.12. Cell proliferation assay

A549 and H1299 cells were transfected as described above, followed by counting and plating at 2.5×10^3/well. Then, 10 μL of CCK-8 (Boiss, China) reagent was added to the adherent A549 and H1299 cells at 0, 24, 48, and 72 h to detect the effects of downregulation of DIP2B expression on cell proliferation. The experiment was performed in triplicate.

2.13. Cell migration and invasion

A549 and H1299 cells were transfected as described above, followed by counting and adjusting the concentration of A549 and H1299 cells. The control group and interference DIP2B expression group cells were added to the upper chamber of the Transwell chamber, with 600 μL of complete medium added to the lower chamber. The chamber was washed with phosphate-buffered saline after 24 h of incubation at 37 °C and 5 % CO_2, and nonmigrating LUAD cells were wiped off the membrane with a cotton swab. Then, migrating A549 and H1299 cells were stained with 0.2 % crystal violet and subsequently counted by ImageJ, and the experiment was performed in triplicate.

2.14. Statistical analysis

The expression of DIP2B in the normal tissues and cancer of LUAD patients and LUAD tissues based on the clinicopathological features was tested by the Wilcoxon rank sum test, chi-square test, and Fisher test, and whether the levels of immune cells in the high- and low-DIP2B expression groups were statistically significant was determined. K–M survival analysis, Cox regression analysis, and meta-analysis of the relationship between DIP2B expression and prognostic indicators in patients with LUAD. A P value < 0.05 was considered significant.

3. Results

3.1. Enhanced DIP2B expression had a poor prognosis in LUAD patients

DIP2B expression was significantly increased in unpaired (Fig. 1A) and paired cancer tissues (Fig. 1B), as well as in cancer patients during the DSS endpoint event (Fig. 1C). The results showed that DIP2B was overexpressed in most cancer tissues of LUAD patients using IHC method (Fig. 1D). Specifically, in 10 LUAD patients, the levels of DIP2B were significantly increased in cancer tissues of 9 of the LUAD patients. In addition, DIP2B expression was associated with OS and DSS in LUAD patients according to the chi-square test

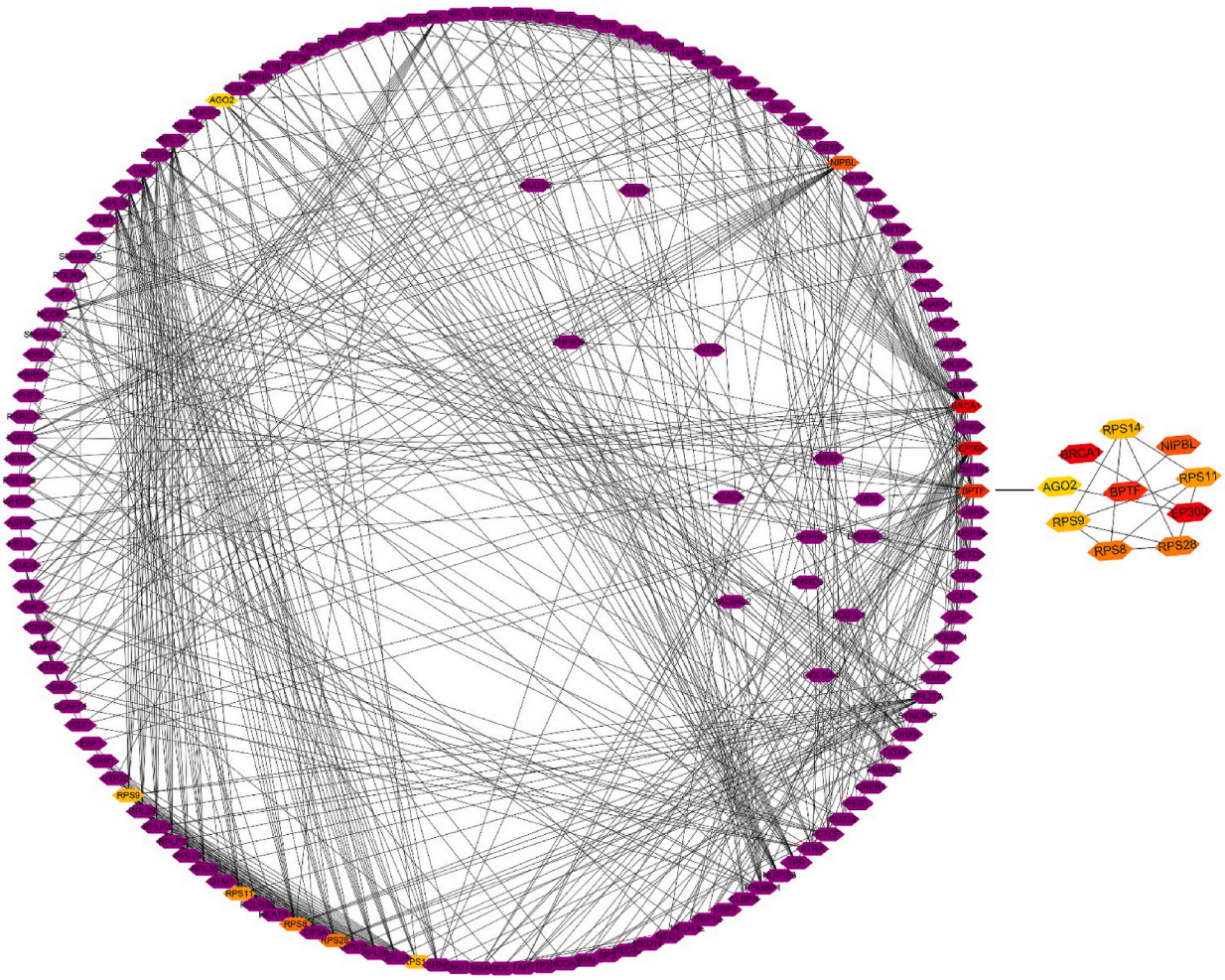

Fig. 8. The key genes in the PPI network. Note: PPI, protein–protein interaction.

(Table 1). The K–M survival method revealed that elevated DIP2B expression was associated with a shorter OS, DSS, and PFI in LUAD patients (Fig. 1E–G). The LUAD patients with high DIP2B expression had a poor prognosis (Fig. 2).

3.2. DIP2B overexpression was associated with a poor prognosis in the LUAD patient subgroup

The K–M survival method revealed that DIP2B overexpression was associated with shorter OS in cancer patients with N0, M0, pathological stage I, pathological stage I-III, R0, age (>65), and no smoking history (Fig. 3). In cancer patients with T1-2, T1-3, N0, M0, pathological stage I, pathological stage I-II, pathological stage I-III, female sex, age (>65), no smoking history, and smoking history, DIP2B overexpression was correlated with a short DSS (Fig. 4). In cancer patients with T1-2, T1-3, N0, pathological stage I, pathological stage I-II, pathological stage I-III, age (>65), and no smoking history, DIP2B overexpression was associated with a shorter PFI (Fig. 5).

3.3. DIP2B-related nomograms

T stage, N stage, and DIP2B overexpression were risk factors for short OS and DSS in LUAD patients (Tables 2 and 3). Fig. 6A and B reveal the association of T stage, N stage, and DIP2B expression with OS and DSS in LUAD patients. T stage, pathological stage, and DIP2B overexpression were risk factors for a short PFI in LUAD patients (Table 4). Fig. 6C reveals the relationship of the T stage, pathological stage, and DIP2B expression with the PFI. Fig. 6D–F shows the calibration curve of nomogram.

3.4. Functions and mechanisms of DIP2B co-expressed genes

There were 640 DIP2B co-expressed genes (Table S1), which were involved in protein binding, RNA binding, cell division, DNA

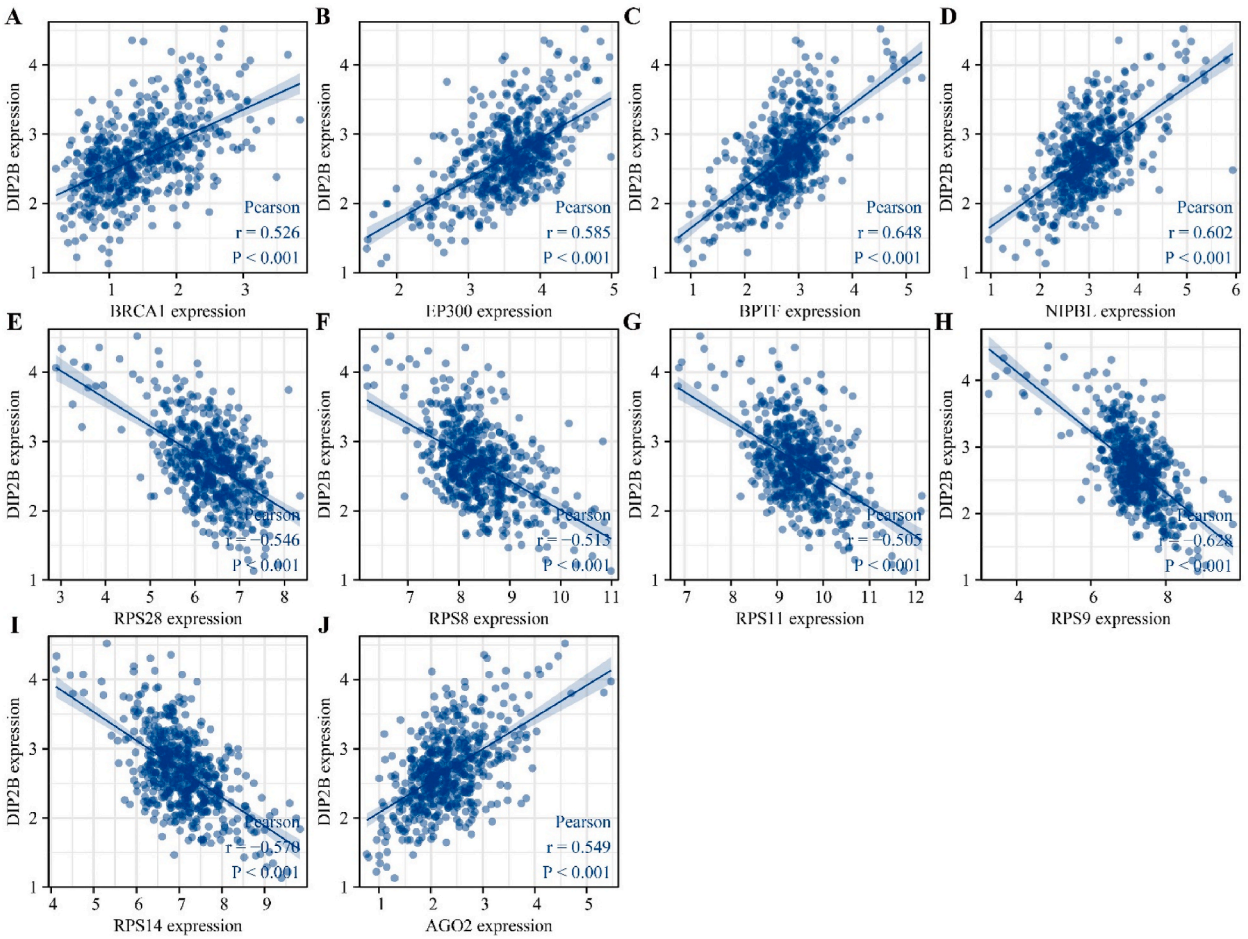

Fig. 9. DIP2B expression was significantly associated with ten hub genes using Pearson correlation analysis. (A) BRCA1; (B) EP300; (C) BPTF; (D) NIPBL; (E) RPS28; (F) RPS8; (G) RPS11; (H) RPS9; (I) RPS14; (J) AGO2.

Table 6
The clinical roles of hub genes in prognosis via K–M survival analysis.

Gene	OS		DSS		PFI	
	HR	P	HR	P	HR	P
BRCA1	1.47 (1.10–1.97)	0.008	1.74 (1.20–2.53)	0.003	1.40 (1.08–1.83)	0.012
EP300	1.03 (0.78–1.38)	0.821	1.31 (0.91–1.89)	0.143	1.15 (0.89–1.50)	0.292
BPTF	1.12 (0.84–1.49)	0.457	1.19 (0.82–1.71)	0.36	1.24 (0.95–1.62)	0.111
NIPBL	0.86 (0.64–1.15)	0.304	1.02 (0.71–1.47)	0.895	0.94 (0.72–1.23)	0.66
RPS28	0.82 (0.62–1.10)	0.185	0.85 (0.59–1.22)	0.384	0.81 (0.63–1.06)	0.126
RPS8	0.84 (0.63–1.12)	0.233	0.81 (0.57–1.17)	0.27	0.79 (0.61–1.03)	0.083
RPS11	1.28 (0.96–1.71)	0.093	1.38 (0.96–1.99)	0.085	1.10 (0.84–1.43)	0.485
RPS9	1.06 (0.80–1.42)	0.672	1.00 (0.70–1.44)	0.998	1.01 (0.77–1.31)	0.957
RPS14	0.86 (0.65–1.15)	0.316	0.82 (0.57–1.18)	0.293	0.86 (0.66–1.13)	0.278
AGO2	1.07 (0.80–1.43)	0.641	1.33 (0.92–1.92)	0.124	1.06 (0.82–1.38)	0.651

Note: LUAD, lung adenocarcinoma; PFI, progression-free survival; OS, overall survival; K–M, Kaplan–Meier; DSS, disease-specific survival; HR, hazard ratio.

repair, protein ubiquitination, chromatin binding, cell cycle, positive transcriptional regulation, etc. (Table S2 and Fig. 7A–C). The KEGG analysis revealed that DIP2B co-expressed genes were involved in ubiquitin-mediated proteolysis, endocrine resistance, ERBB signaling pathway, cell cycle, chemical carcinogenesis-reactive oxygen species, viral carcinogenesis, EGFR tyrosine kinase inhibitor resistance, and other mechanisms (Table 5 and Fig. 7D).

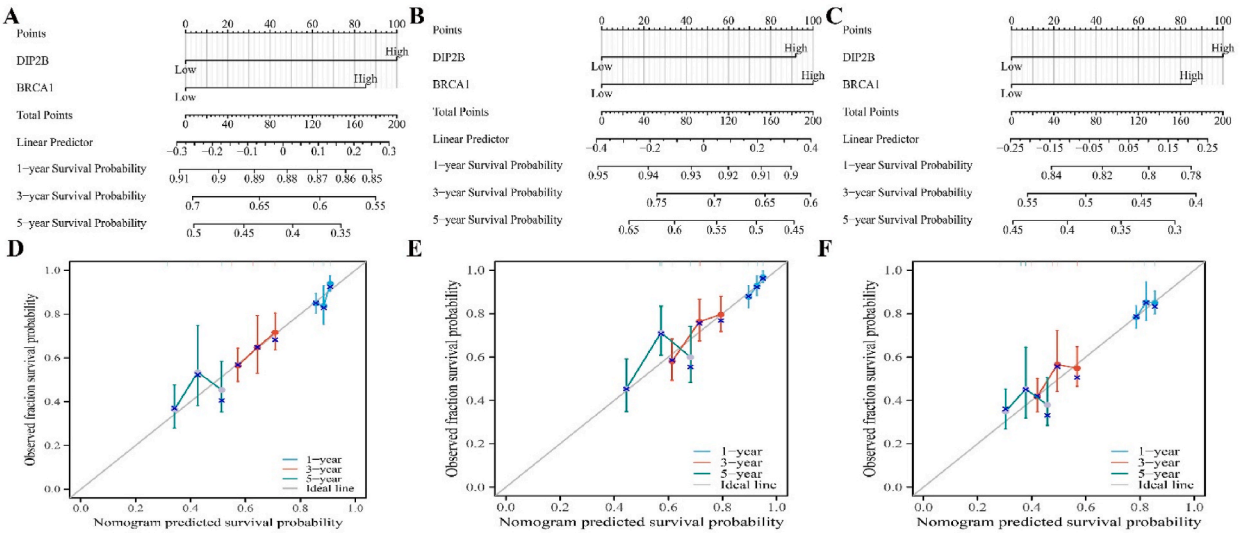

Fig. 10. The nomograms of DIP2B and BRCA1 overexpression predicted the dismal prognosis of LUAD patients at 1, 3, and 5 years. (A) OS-related nomogram; (B) DSS-related nomogram; (C) PFI-related nomogram; (D–F) The calibration curves of nomogram in OS, DSS, and PFI.Note: LUAD, lung adenocarcinoma; PFI, progression-free survival; OS, overall survival; DSS, disease-specific survival.

3.5. DIP2B was significantly associated with key genes in the PPI network

We constructed a PPI network of DIP2B co-expressed genes through the STRING database (Fig. S1). Fig. 8 reveals the key genes in the PPI network of DIP2B co-expressed genes using the CytoHubba plugin, and the key genes were BRCA1, EP300, BPTF, NIPBL, RPS28, RPS8, RPS11, RPS9, RPS14, and AGO2. The expression of DIP2B was positively correlated with the expression of BRCA1, EP300, BPTF, NIPBL, and AGO2 and negatively correlated with the expression of RPS28, RPS8, RPS11, RPS9, and RPS14 (Fig. 9).

3.6. Nomograms of DIP2B co-expressed genes

The expression of the hub gene BRCA1 was associated with the prognosis of LUAD patients (Table 6). Specifically, BRCA1 overexpression was significantly associated with shorter OS, DSS, and PFI in cancer patients, with hazard ratios (HRs) of 1.47, 1.74, and 1.4, respectively. The relationship between DIP2B and the co-expressed gene BRCA1 and the OS, DSS, and PFI at 1, 3, and 5 years of LUAD patients was determined using nomograms (Fig. 10A-C). In short, 1-, 3-, and 5-year survival times, DSS, and PFI were poorer in LUAD patients with DIP2B and BRCA1 overexpression. Fig. 10D–F shows the calibration curve of nomogram.

3.7. Inhibition of DIP2B expression downregulated LUAD cell growth and migration ability

DIP2B protein expression was inhibited in A549 and H1299 cells by siRNA interference technology (Fig. 11A) and inhibition of DIP2B significantly downregulated the proliferation ability of LUAD cells (Fig. 11B–C). The proliferation ability of the si-DIP2B experimental and control groups was significantly different at 48 and 72 h, without a significant difference between the si-DIP2B experimental groups. In addition, decreased DIP2B expression was accompanied by decreased LUAD cell migration (Fig. 11D–G and 12A-D). The results of western blotting showed that inhibition of DIP2B expression downregulated CCND1 and MMP2 protein expression (Fig. 12E and F). Preliminary evidence suggested that DIP2B functions as an oncogene, and inhibition of DIP2B expression decreased the growth, migration and invasiveness of LUAD cells *in vitro*.

3.8. The expression of DIP2B was related to the immune microenvironment in LUAD

DIP2B expression was positively correlated with the levels of Central Memory T-cell (Tcm) ($r = 0.397$), T helper cells ($r = 0.3$), T helper 2 (Th2) cells ($r = 0.276$), Effective Memory T-Cell (Tem) ($r = 0.16$), and Tgd ($r = 0.146$), and negatively correlated with the levels of CD8 T cells ($r = -0.418$), Immature Dendritic Cells (iDCs) ($r = -0.322$), Natural killer (NK) CD56bright cells ($r = -0.286$), Follicular helper T-cell (TFH) ($r = -0.281$), plasmacytoid Dendritic Cells (pDC) ($r = -0.260$), mast cells ($r = -0.258$), Dendritic Cells (DC) ($r = -0.254$), cytotoxic cells ($r = -0.231$), Regulatory T cells (TReg) ($r = -0.217$), NK cells ($r = -0.205$), T helper 17 (Th17) cells ($r = -0.199$), B cells ($r = -0.179$), T helper 1 (Th1) cells ($r = -0.166$), macrophages ($r = -0.117$), eosinophils ($r = -0.116$), T cells ($r = -0.114$), and activated DCs (aDC) ($r = -0.11$) in LUAD (Figs. S2 and 13). The DC, iDC, NK CD56bright cells, B cells, CD8 T cells, cytotoxic cells, macrophages, mast cells, pDCs, T cells, T helper cells, Tcm, TFH, Tgd, Th1 cells, Th17 cells, Th2 cells, and TReg levels were significantly different between the high- and low-DIP2B expression groups (Fig. S3). In addition, the expression of DIP2B was

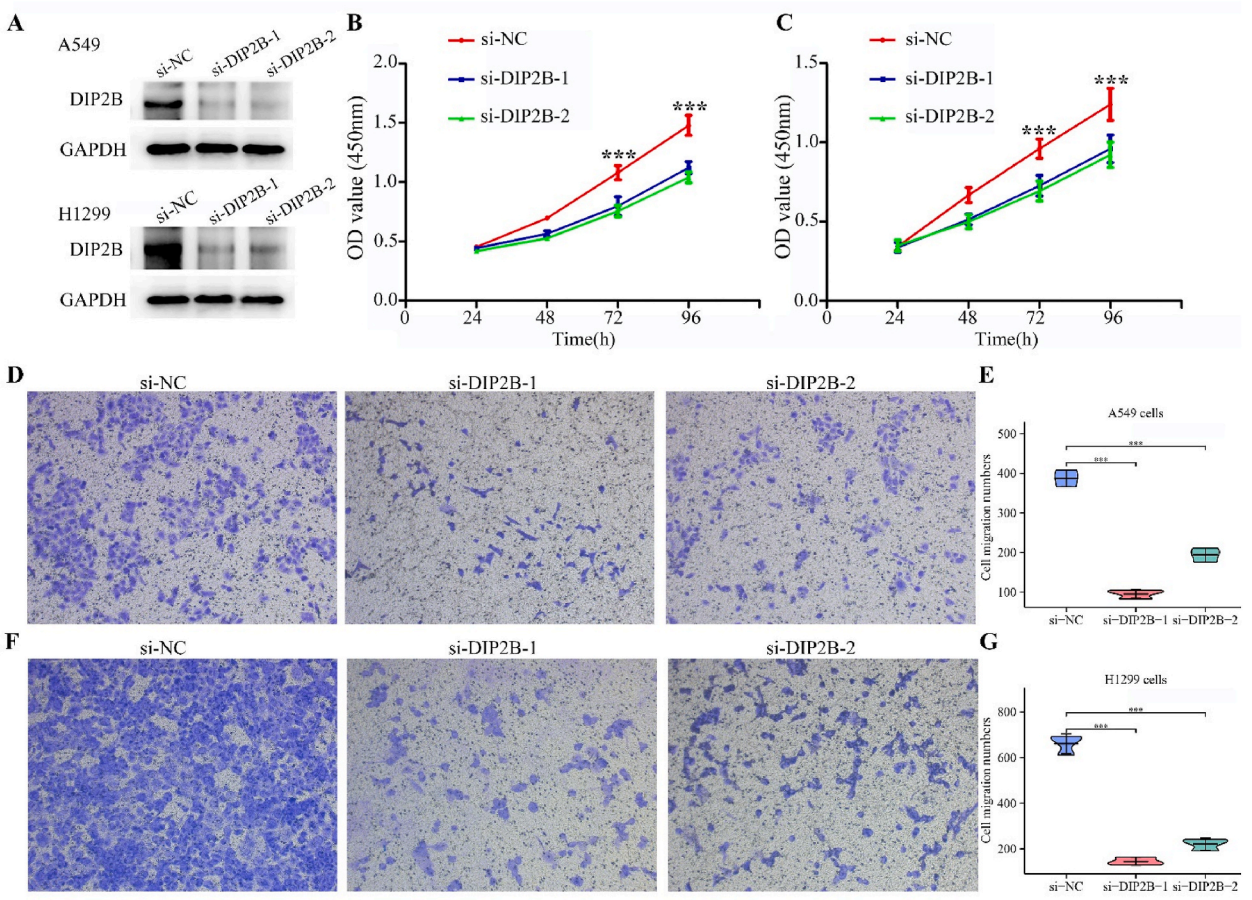

Fig. 11. Inhibition of DIP2B expression downregulates LUAD cell proliferation and migration. (A) Identification of cell models using western blotting; (B–C) Cell proliferation of A549 and H1299 cells using CCK-8; (D) A549 cell migration using a transwell assay; (E) Whether the migration of A549 cells is differentially affected by DIP2B expression is determined using statistical analysis; (F) H1299 cell migration using a transwell assay; (G) Whether the migration of H1299 cells is differentially affected by DIP2B expression is determined using statistical analysis. Note: LUAD, lung adenocarcinoma; ***, $P < 0.001$.

correlated with the levels of HLA-DPB1, HLA-DRA, CD1C, STAT1, HLA-DQB1, STAT3, HLA-DPA1, STAT5B, CD3D, TGFB1, CD163, CCR8, CD79A, etc (Table 7 and Fig. 14).

4. Discussion

Recently, reducing the morbidity and mortality of LUAD has been a major global public health concern. Some biomarkers could predict the survival time of LUAD patients and inhibit or promote the progression of LUAD [19–22]. EHD2 protein expression is decreased in LUAD and is associated with lymph node metastasis, advanced tumor stage, and decreased survival, as well as being an independent prognostic factor in cancer patients. Inhibition of EHD2 expression promoted the migration and invasion of A549 cells. Overexpression of EHD2 inhibited the migration and invasion of H1299 cells [19]. The expression of DDR1 in LUAD tissues is higher than that in normal tissues, and DDR1 overexpression is negatively correlated with poor prognosis in LUAD patients. DDR1 promoted cancer cell migration and invasion *in vitro* and altered the expression of markers of the epithelial-mesenchymal transition process [22]. In the present study, DIP2B was overexpressed in unpaired and paired LUAD tissues based on TCGA database analysis and clinical tissue samples and was associated with shorter OS, DSS, and PFI in LUAD patients. Univariate Cox regression analysis, multivariate Cox regression analysis, and the nomograms showed that DIP2B overexpression was a risk factor for short prognostic indicators in patients with LUAD, indicating that DIP2B is a potential biomarker of poor prognosis in LUAD patients.

The cell cycle is an important link in cancer progression. Oncogenes or suppressor genes are involved in cancer progression by affecting the cell cycle [23–25]. For example, CDCA5 is associated with the occurrence and development of NSCLC and is a biomarker for predicting the prognosis of patients with early-stage LUAD. Silencing CDCA5 expression could induce cell cycle arrest and increase apoptosis [24]. PTBP3 expression is significantly increased in lung squamous cell carcinoma (LUSC), and elevated PTBP3 expression predicts a poor prognosis in patients with LUSC. *In vitro* and *in vivo* studies have revealed that inhibition of PTBP3 expression decreases

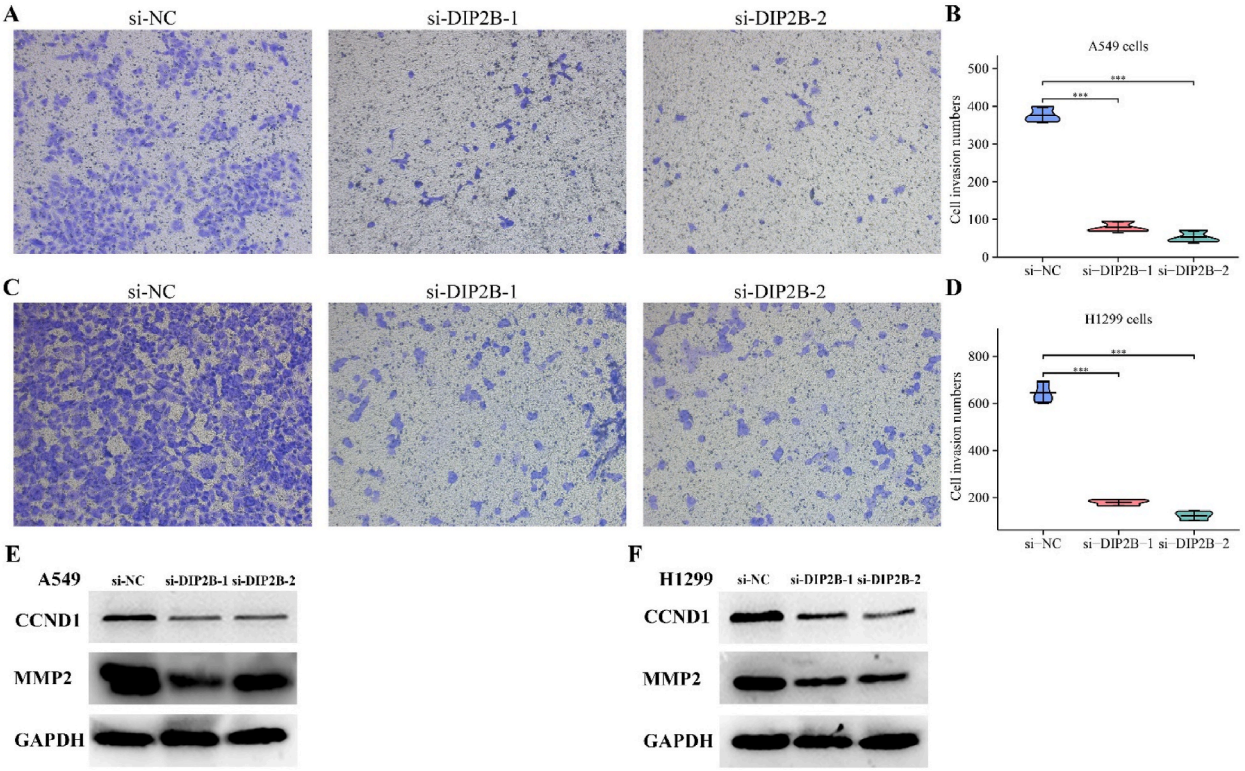

Fig. 12. Inhibition of DIP2B expression hinders the invasiveness and cell cycle-related protein expression of LUAC cells. (A) A549 cell invasive ability; (B) Whether the invasive ability of A549 cells is differentially affected by DIP2B expression is determined using statistical analysis; (C) H1299 cell invasive ability; (B) Whether the invasive ability of H1299 cells is differentially affected by DIP2B expression is determined using statistical analysis; (E and F) Inhibition of DIP2B expression downregulates CCND1 and MMP2 protein expression.Note: LUAD, lung adenocarcinoma; ***, $P < 0.001$.

cell proliferation and prevents cell cycle progression by reducing the CDK2/Cyclin A2 complex [25]. In our A549 and H1299 cell models, suppressed DIP2B expression was accompanied by decreased LUAD cell proliferation, migration, and invasion abilities. KEGG results showed that DIP2B was involved in DNA repair and the cell cycle. In addition, the decreased expression of DIP2B could inhibit the expression of CCND1 and MMP2 using western blotting. These results further suggest that decreased expression of DIP2B could inhibit LUAD progression by affecting the expression of CCND1 and MMP2 protein.

At present, nomograms are often used to display the relationship between prognostic factors and the survival time of cancer patients [26–28]. For example, nine telomere-related genes (TRGs), ABCC2, ABCC8, ALDH2, FOXP3, GNMT, JSRP1, MACF1, PLCD3, and SULT4A1, were abnormally expressed in LUAD tissues. A nomogram constructed based on the TRG gene could predict the survival time of LUAD patients [26]. We found that the expression of DIP2B was positively correlated with the expression of co-expressed gene BRCA1. Overexpression of co-expressed gene BRCA1 was significantly associated with shorter OS, DSS, and PFI in cancer patients, with hazard ratios (HRs) of 1.47, 1.74, and 1.4, respectively. The relationship between DIP2B and the hub gene BRCA1 and the OS, DSS, and PFI at 1, 3, and 5 years of LUAD patients was determined using nomograms. In short, 1-, 3-, and 5-year survival times, DSS, and PFI were poorer in LUAD patients with DIP2B and BRCA1 overexpression. DIP2B- and BRCA1-related nomograms might be useful tools for predicting the prognosis of LUAD patients.

The immune microenvironment contains immune cells, inflammatory cells, signaling molecules, etc. An abnormal immune microenvironment often leads to tumorigenesis or cancer progression [29–33]. CXCL13 is overexpressed in high-grade serous ovarian cancer tissues. Elevated CXCL13 expression prolonged patient survival and was positively correlated with tumor activation and CXCR5CD8 T-cell infiltration. CXCL13 was associated with CD20 B-cell clusters, and CD20 B cells could predict better survival of cancer patients when CXCL13 was expressed. CXCL13 combined with anti-PD-1 therapy delayed cancer growth in a CD8 T-cell-dependent manner, resulting in the infiltration of cytotoxic CD8 T cells and CXCR5 CD8 T cells [31]. In our study, DIP2B expression was positively correlated with the levels of Tcm, T helper cells, Th2 cells, Tem and Tgd and negatively correlated with the levels of CD8 T cells, iDCs, NK CD56bright cells, TFH, and others in LUAD. In addition, the expression of DIP2B was related to immune cell markers (such as HLA-DPB1, HLA-DRA, CD1C, STAT1, HLA-DQB1, STAT3, HLA-DPA1, STAT5B, CD3D, TGFB1, CD163, CCR8, and CD79A), indicating that overexpression of DIP2B was related to the LUAD immune microenvironment. However, the roles of DIP2B in the immune microenvironment of LUAD should be confirmed in the future.

We found that DIP2B overexpression was observed in LUAD using both LUAD samples from the TCGA database and clinical

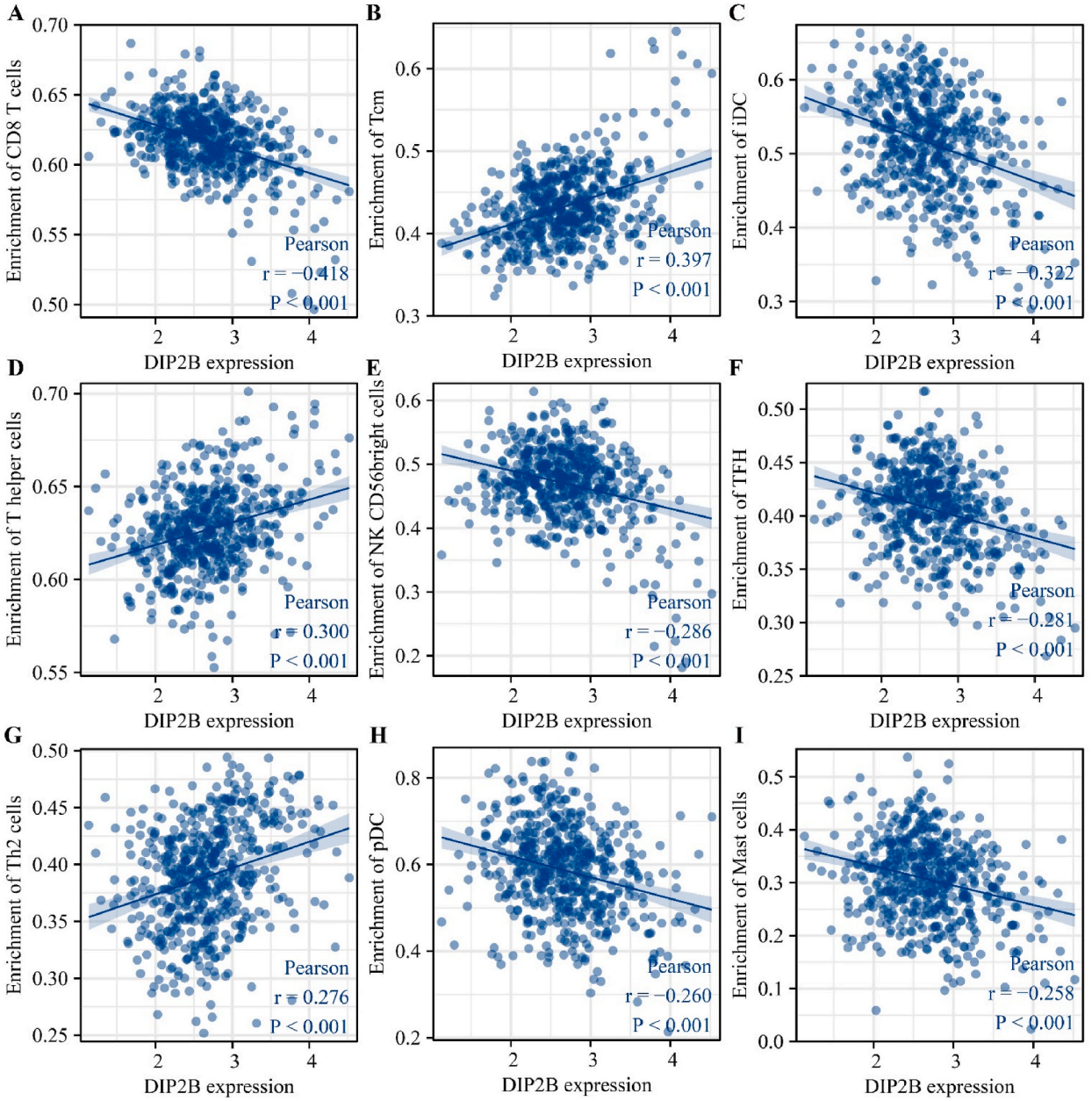

Fig. 13. DIP2B expression is related to immune cells in LUAD according to Pearson correlation analysis. (A) CD8 T cells; (B) Tcms; (C) iDCs; (D) T helper cells; (E) NK CD56bright cells; (F) TFH cells; (G) Th2 cells; (H) pDCs; (I) mast cells. Note: LUAD, lung adenocarcinoma.

Table 7
DIP2B expression is related to immune cell markers in LUAD using Pearson correlation analysis.

Markers	Immune cells	Correlation coefficient	P value
HLA-DPB1	Dendritic cells	−0.330	<0.001
HLA-DRA	Dendritic cells	−0.317	<0.001
CD1C	Dendritic cells	−0.304	<0.001
HLA-DQB1	Dendritic cells	−0.272	<0.001
HLA-DPA1	Dendritic cells	−0.223	<0.001
NRP1	Dendritic cells	0.093	0.032
IFNG	Th1 cells	0.124	0.004
STAT1	Th1 cells	0.295	<0.001
GATA3	Th2 cells	0.136	0.002
STAT3	Th17 cells	0.266	<0.001
CCR8	Treg	0.170	<0.001
TGFB1	Treg	−0.186	<0.001
STAT5B	Treg	0.204	<0.001
CD3D	T cell (general)	−0.198	<0.001
CD3E	T cell (general)	−0.143	<0.001
CD2	T cell (general)	−0.108	0.012
PTGS2	M1 Macrophage	0.108	0.012
NOS2	M1 Macrophage	0.096	0.027
CD163	M2 Macrophage	0.178	<0.001
IL21	Tfh	0.132	0.002
CD68	TAM	−0.113	0.009
CEACAM8	Neutrophils	−0.104	0.016

Note: LUAD, lung adenocarcinoma.

patients, providing the benefits of ample patient samples and reliable data. In addition, inhibiting the expression of DIP2B could delay the proliferation, migration and invasion of LUAD cells, resulting in a decrease in the expression of CCND1 and MMP2. The results of basic research and clinical tissues *in vitro* were consistent with the results of database analysis. This provides a new candidate molecule for the treatment of LUAD patients. This study also has the following deficiencies. The roles and signaling mechanisms of DIP2B expression in nude mice and the roles of DIP2B in the immune microenvironment, antitumor immune response, and immunotherapy of LUAD should be explored in the future by collecting more LUAD tissue samples and conducting basic *in vitro* experiments. In general, inhibiting DIP2B expression downregulated cancer cell growth and migration, which might be related to the decrease in CCND1 and MMP2 protein expression. DIP2B-related nomograms might be useful tools for predicting the prognosis of LUAD patients.

5. Conclusion

The present results indicate that DIP2B has an important biological role in LUAD progression and is associated with the immune microenvironment in LUAD. Studies have shown that inhibition of DIP2B expression could retard LUAD growth and metastasis using CCND1 and MMP2 expression. Thus, DIP2B is a potential prognostic biomarker for LUAD patients, but further studies are required to validate the clinical value of DIP2B.

Data availability

The study data are available upon request from the corresponding authors.

Funding

This research was funded via the Natural Science Foundation of China (No. 82100115 and 82100299), the Health Commission of Hubei Provincial (No. WJ2023M166), and the Natural Science Foundation of Hubei (No. 2024AFB694).

Ethical approval

Written informed consent was obtained from all LUAD patients in our hospital, and this study was approved by the Ethics Committee of Huazhong University of Science and Technology.

CRediT authorship contribution statement

Chuang-Yan Wu: Writing – original draft, Visualization, Methodology, Investigation. **Zhao Liu:** Writing – original draft, Investigation, Data curation. **Wei-Min Luo:** Writing – original draft, Visualization, Investigation, Data curation. **Huan Huang:** Investigation, Data curation, Validation, Visualization. **Ni Jiang:** Visualization, Software, Methodology, Data curation. **Zhi-Peng Du:** Validation, Methodology, Formal analysis. **Fang-Ming Wang:** Methodology, Investigation, Data curation. **Xu Han:** Validation,

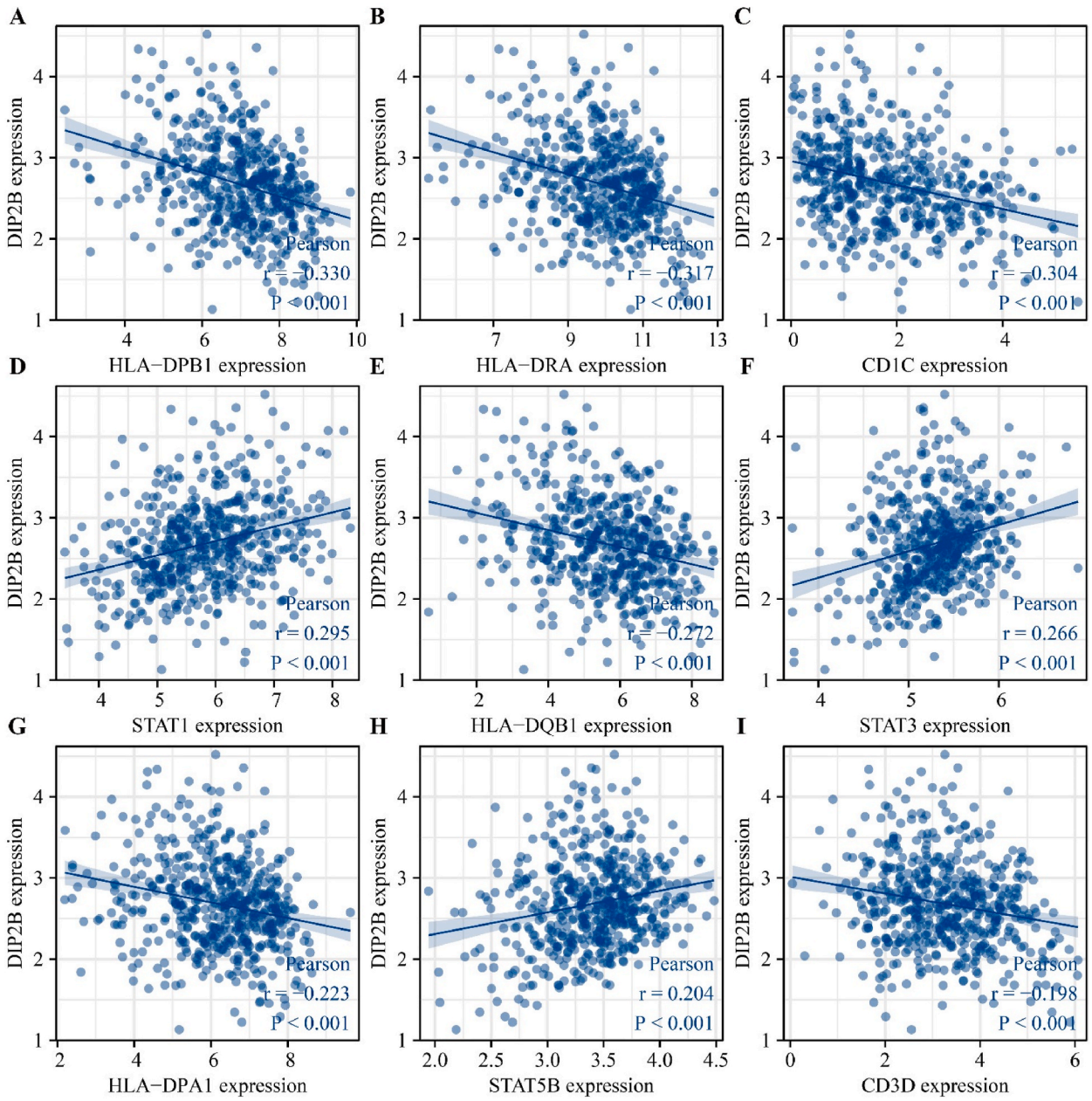

Fig. 14. DIP2B expression is related to immune cell markers in LUAD using Pearson correlation analysis. (A) HLA-DPB1; (B) HLA-DRA; (C) CD1C; (D) STAT1; (E) HLA-DQB1; (F) STAT3; (G) HLA-DPA1; (H) STAT5B; (I) CD3D.Note: LUAD, lung adenocarcinoma.

Methodology. **Guan-Chao Ye:** Supervision, Software, Investigation. **Qiang Guo:** Writing – review & editing, Data curation, Conceptualization. **Jiu-Ling Chen:** Writing – review & editing, Supervision, Data curation, Conceptualization.

Declaration of competing interest

There is no conflict of interest in this research.

Acknowledgment

We are grateful to the TCGA database for providing open data on LAC patients and thank Home for Researchers editorial team (www.home-forresearchers.com) for language editing service.

Appendix A. Supplementary data

Supplementary data to this article can be found online at https://doi.org/10.1016/j.heliyon.2024.e32025.

References

[1] N. Liang, S. Sun, Z. Li, et al., CCKAR is a biomarker for prognosis and asynchronous brain metastasis of non-small cell lung cancer, Front Oncol 12 (2023) 1098728, https://doi.org/10.3389/fonc.2022.1098728.

[2] Y.Q. Zhang, Y. Yuan, J. Zhang, et al., Evaluation of the roles and regulatory mechanisms of PD-1 target molecules in NSCLC progression, Ann Transl Med 9 (2021) 1168, https://doi.org/10.21037/atm-21-2963.

[3] H. Zhang, D. Jiang, H. Jin, et al., Novel mutation signatures in the prognosis of EGFR-TKIs targeted therapy for non-small cell lung cancer patients based on the 1000-gene panel sequencing, Neoplasma 69 (2022) 352–360, https://doi.org/10.4149/neo_2021_210914N1307.

[4] L.B. Cameron, N. Hitchen, E. Chandran, et al., Targeted therapy for advanced anaplastic lymphoma kinase (*ALK*)-rearranged non-small cell lung cancer, Cochrane Database Syst Rev 1 (2022) CD013453, https://doi.org/10.1002/14651858.CD013453.pub2.

[5] Y. Yuan, J. Bao, Z. Chen, et al., Multi-omics analysis to identify susceptibility genes for colorectal cancer, Hum Mol Genet 30 (2021) 321–330, https://doi.org/10.1093/hmg/ddab021.

[6] S. Adlat, F. Hayel, Y. Chen, et al., Heterozygous loss of Dip2B enhances tumor growth and metastasis by altering immune microenvironment, Int Immunopharmacol 105 (2022) 108559, https://doi.org/10.1016/j.intimp.2022.108559.

[7] R.K. Sah, J. Ma, F.B. Bah, et al., Targeted disruption of mouse Dip2B leads to abnormal lung development and prenatal lethality, Int J Mol Sci 21 (2020) 8223, https://doi.org/10.3390/ijms21218223.

[8] S. Adlat, R.K. Sah, F. Hayel, et al., Global transcriptome study of Dip2B-deficient mouse embryonic lung fibroblast reveals its important roles in cell proliferation and development, Comput Struct Biotechnol J 18 (2020) 2381–2390, https://doi.org/10.1016/j.csbj.2020.08.030.

[9] Q. Guo, X.X. Ke, Z. Liu, et al., Evaluation of the prognostic value of STEAP1 in lung adenocarcinoma and insights into its potential molecular pathways via bioinformatic analysis, Front Genet 11 (2020) 242, https://doi.org/10.3389/fgene.2020.00242.

[10] S. Tong, N. Jiang, J.H. Wan, et al., The effects of the prognostic biomarker SAAL1 on cancer growth and its association with the immune microenvironment in lung adenocarcinoma, BMC Cancer 23 (2023) 275, https://doi.org/10.1186/s12885-023-10741-5.

[11] Z. He, S. Wang, J. Wu, et al., Lower expression of TWEAK is associated with poor survival and dysregulate TIICs in lung adenocarcinoma, Dis Markers 2022 (2022) 8661423, https://doi.org/10.1155/2022/8661423.

[12] N. Zhu, Y. Yang, H. Wang, et al., CSF2RB is a unique biomarker and correlated with immune infiltrates in lung adenocarcinoma, Front Oncol 12 (2022) 822849, https://doi.org/10.3389/fonc.2022.822849.

[13] D. Li, X. Liu, N. Jiang, et al., Interfering with ITGB1-DT expression delays cancer progression and promotes cell sensitivity of NSCLC to cisplatin by inhibiting the MAPK/ERK pathway, Am J Cancer Res 12 (2022) 2966–2988.

[14] Q.M. Xiang, N. Jiang, Y.F. Liu, et al., Overexpression of SH2D1A promotes cancer progression and is associated with immune cell infiltration in hepatocellular carcinoma via bioinformatics and in vitro study, BMC Cancer 23 (2023) 1005, https://doi.org/10.1186/s12885-023-11315-1.

[15] F.M. Wang, L.Q. Xu, Z.C. Zhang, et al., SLC7A8 overexpression inhibits the growth and metastasis of lung adenocarcinoma and is correlated with a dismal prognosis, Aging (Albany NY) 16 (2024) 1605–1619, https://doi.org/10.18632/aging.205446.

[16] X. Zhang, D. Jiang, S. Li, et al., A signature-based classification of lung adenocarcinoma that stratifies tumor immunity, Front Oncol 12 (2023) 1023833, https://doi.org/10.3389/fonc.2022.1023833.

[17] Q. Guo, C.Y. Wu, N. Jiang, et al., Downregulation of T-cell cytotoxic marker IL18R1 promotes cancer proliferation and migration and is associated with dismal prognosis and immunity in lung squamous cell carcinoma, Front Immunol 13 (2022) 986447, https://doi.org/10.3389/fimmu.2022.986447.

[18] H.S. Liu, Q. Guo, H. Yang, et al., SPDL1 overexpression is associated with the 18F-fdg PET/CT metabolic parameters, prognosis, and progression of esophageal cancer, Front Genet 13 (2022) 798020, https://doi.org/10.3389/fgene.2022.798020.

[19] S. Wei, J. Shao, J. Wang, et al., EHD2 inhibits the invasive ability of lung adenocarcinoma and improves the prognosis of patients, J Thorac Dis 14 (2022) 2652–2664, https://doi.org/10.21037/jtd-22-842.

[20] J. Wang, Y. Yuan, L. Tang, et al., Long non-coding RNA-TMPO-AS1 as ceRNA binding to let-7c-5p upregulates STRIP2 expression and predicts poor prognosis in lung adenocarcinoma, Front Oncol 12 (2022) 921200, https://doi.org/10.3389/fonc.2022.921200.

[21] R. Yiminniyaze, X. Zhang, N. Zhu, et al., EphrinA3 is a key regulator of malignant behaviors and a potential prognostic factor in lung adenocarcinoma, Cancer Med 12 (2023) 1630–1642, https://doi.org/10.1002/cam4.4987.

[22] J. Zhu, H. Cheng, L. Wang, et al., Discoidin domain receptor 1 promotes lung adenocarcinoma migration via the AKT/snail signaling axis, Mol Biol Rep 49 (2022) 7275–7286, https://doi.org/10.1007/s11033-022-07509-8.

[23] J. Lee, K. Kim, T.Y. Ryu, et al., EHMT1 knockdown induces apoptosis and cell cycle arrest in lung cancer cells by increasing CDKN1A expression, Mol Oncol 15 (2021) 2989–3002, https://doi.org/10.1002/1878-0261.13050.

[24] W. Shen, D. Tong, J. Chen, et al., Silencing oncogene cell division cycle associated 5 induces apoptosis and G1 phase arrest of non-small cell lung cancer cells via p53-p21 signaling pathway, J Clin Lab Anal 36 (2022) e24396, https://doi.org/10.1002/jcla.24396.

[25] Y. Chen, Y. Ji, S. Liu, et al., PTBP3 regulates proliferation of lung squamous cell carcinoma cells via CDC25A-mediated cell cycle progression, Cancer Cell Int 22 (2022) 19, https://doi.org/10.1186/s12935-022-02448-7.

[26] H. Chen, W. Liang, W. Zheng, et al., A novel telomere-related gene prognostic signature for survival and drug treatment efficiency prediction in lung adenocarcinoma, Aging (Albany NY) 15 (2023) 7956–7973, https://doi.org/10.18632/aging.204877.

[27] H. Li, X. Sha, W. Wang, et al., Identification of lysosomal genes associated with prognosis in lung adenocarcinoma, Transl Lung Cancer Res 12 (2023) 1477–1495, https://doi.org/10.21037/tlcr-23-14.

[28] Q. Guo, Y.Y. Peng, H. Yang, et al., Prognostic nomogram for postoperative patients with gastroesophageal junction cancer of No distant metastasis, Front Oncol 11 (2021) 643261, https://doi.org/10.3389/fonc.2021.643261.

[29] L. Qi, C. Ye, D. Zhang, et al., The effects of differentially-expressed homeobox family genes on the prognosis and HOXC6 on immune microenvironment orchestration in colorectal cancer, Front Immunol 12 (2021) 781221, https://doi.org/10.3389/fimmu.2021.781221.

[30] Y. Li, C. Lv, Y. Yu, et al., KIR3DL3-HHLA2 and TMIGD2-HHLA2 pathways: the dual role of HHLA2 in immune responses and its potential therapeutic approach for cancer immunotherapy, J Adv Res 47 (2023) 137–150, https://doi.org/10.1016/j.jare.2022.07.013.

[31] M. Yang, J. Lu, G. Zhang, et al., CXCL13 shapes immunoactive tumor microenvironment and enhances the efficacy of PD-1 checkpoint blockade in high-grade serous ovarian cancer, J Immunother Cancer 9 (2021) e001136, https://doi.org/10.1136/jitc-2020-001136.

[32] K. Tsuchiya, K. Yoshimura, Y. Inoue, et al., YTHDF1 and YTHDF2 are associated with better patient survival and an inflamed tumor-immune microenvironment in non-small-cell lung cancer, Oncoimmunology 10 (2021) 1962656, https://doi.org/10.1080/2162402X.2021.1962656.

[33] H. Zhang, Z. Liu, H. Wen, et al., Immunosuppressive TREM2(+) macrophages are associated with undesirable prognosis and responses to anti-PD-1 immunotherapy in non-small cell lung cancer, Cancer Immunol Immunother 71 (2022) 2511–2522, https://doi.org/10.1007/s00262-022-03173-w.